Articles

Characterization of DNA−Protein Cross-Links Induced by Oxanine: Cellular Damage Derived from Nitric Oxide and Nitrous Acid†

Hauh-Jyun Candy Chen,* Chia-Jong Hsieh, Li-Ching Shen, and Chia-Ming Chang

Department of Chemistry and Biochemistry, National Chung Cheng University, 168 University Road, Ming-Hsiung, Chia-Yi 62142, Taiwan

Received September 30, 2006; Revised Manuscript Received January 15, 2007

ABSTRACT: Reactive nitrogen species are implicated in inflammatory diseases and cancers. Oxanine (Oxa) is a DNA lesion derived from the guanine base with nitric oxide, nitrous acid, or *N*-nitrosoindoles. It was shown by gel electrophoresis that oxanine mediated the formation of DNA−protein cross-links (DPCs) with DNA-binding proteins and in the cell extract. Although 2′-deoxyoxanosine was shown to react with amines including the *N*-terminal amino group of glycine, the structures of DNA−protein cross-links induced by oxanine have not been characterized. In this study, we find that the thiol group of the amino acid side chain is reactive toward oxanine, forming a thioester. Two reaction products of oxanine, namely, the thioester and the amide adducts, with the endogenous tripeptide glutathione (GSH) as a model protein were characterized on the basis of their UV, NMR (^{1}H- and ^{13}C-), and mass spectra. Interestingly, the disulfide GSSG also reacts with oxanine, forming the thioester adduct. The thioester and the amide adducts are generated when GSH and GSSG react with oxanine-containing calf thymus DNA, and they might be possible forms of cellular DPCs. Because the repair mechanism of DPCs is not extensively investigated, the characterization of oxanine-derived DPC structures should shed light on their detection *in vivo* and on their biological consequences.

Low concentrations of nitric oxide (NO[1]) are essential to normal physiological functions. However, excessive *in vivo* production of reactive nitrogen oxide species (RNOx), including NO, in inflamed tissues has been proposed to damage DNA and thus play an important role in cancers related to chronic infections and inflammation (*1*, *2*). In particular, reaction of NO with DNA leads to base deamination and oxidation, DNA strand breaks, abasic site formation, and DNA cross-links (*3*−*7*). Nitric oxide is metabolized *in vivo* to nitrite, which can be protonated to nitrous acid (HNO_2) in the acidic environments of phagocytes and lysozymes. The formation and reactivity of HNO_2 may account for an important part of the bactericidal activity of phagocytes (*8*, *9*). Reaction of DNA with NO or HNO_2 leads to the formation of oxanine (5-amino-3*H*-imidazo[4,5-*d*][1,3]-oxazin-7-one, Oxa) as a novel rearrangement product derived from guanine bases in addition to the deamination product xanthine (*7*, *10*). Furthermore, the mutagenic *N*-nitrosoindoles also generate oxanine because of the transfer of the nitroso group to DNA (*11*, *12*).

Oxanine was found to possess mutagenic effects, causing instability of the DNA double helix structure and misincorporation during DNA replication (*13*, *14*). Furthermore, it was shown by gel electrophoresis that oxanine mediated the formation of DNA−protein cross-links (DPCs) with DNA-binding proteins and in the cell extract (*15*). Although 2′-deoxyoxanosine (dOxo) reacts with the N-terminal amino group of glycine (*16*), the structures of DPCs induced by oxanine are not characterized. Although oxanine on DNA can be repaired by base and nucleotide excision repair pathways to a small extent (*17*−*20*), the repair of oxanine-derived DPCs is not extensively investigated.

The formation of the adduct between dOxo and glycine or polyamine (*15*, *16*) suggests that the carbonyl group of Oxa is susceptible to attack by nucleophiles. It is reasonable

† This work was supported by National Science Council of Taiwan (grants NSC 92-2113-M-194-025, NSC 93-2113-M-194-017, and NSC 94-2113-M-194-014) and National Chung Cheng University (to H.-J. C. C.).

* To whom correspondence should be addressed. Tel: (886) 5-242-8176. Fax: (886) 5-272-1040. E-mail: chehjc@ccu.edu.tw.

[1] Abbreviations: BER, base excision repair; CID, collision-induced dissociation; NAc, *N*-acetyl; dOxo, 2′-deoxyoxanosine (5-amino-3-β-D-2′-deoxyribofuranosyl)-3*H*-imidazo[4,5-*d*][1,3]oxazine-7-one); dR, 2-deoxyribose; DTPA, diethylenetriamine pentaacetic acid; DDT, dithiothreitol; ESI/MS, electrospray ionization mass spectrometry; NSI/MS/MS, nanospray ionization tandem mass spectrometry; GSH, reduced glutathione; GSSG, oxidized glutathione disulfide; HMQC, heteronuclear multiple quantum coherence; NER, nucleotide excision repair; NMR, nuclear magnetic resonance; NO, nitric oxide; Oxa, oxanine (5-amino-3*H*-imidazo[4,5-*d*][1,3]oxazin-7-one); Oxa-*N*-GSH, 4-[1-(carboxymethyl-carbamoyl)-2-mercaptoethylcarbamoyl]-2-[(5-ureido-1*H*-imidazole-4-carbonyl)-amino]-butyric acid; Oxa-*S*-GSH, 2-amino-4-[1-(carboxymethyl-carbamoyl)-2-(5-ureido-1*H*-imidazole-4-carbonylsulfanyl)-ethylcarbamoyl]-butyric acid; Oxa-*S*-GSSG, 4-[2-[2-(4-amino-4-carboxy-butyrylamino)-2-(carboxymethyl-carbamoyl)-ethyldisulfanyl]-1-(carboxymethyl-carbamoyl)-ethylcarbamoyl]-2-[(5-ureido-1*H*-imidazole-4-carbonyl)-amino]-butyric acid; RNOx, reactive nitrogen oxide species.

10.1021/bi0620398 CCC: $37.00
Published on Web 03/14/2007

to assume that the nucleophilic side chains of the amino acid residues in protein react with dO on DNA, forming DPCs. In this study, we examine the reactivity of various amino acid side chains with dOxo and find that the thiol group of the amino acid side chain is the most reactive toward oxanine, forming a thioester. Thus, the cysteine residue of proteins might react with the oxanine moiety on DNA, forming DPCs. Using the endogenous tripeptide glutathione (GSH, γGlu-Cys-Gly) as a model protein, we characterize two products of oxanine reacting with GSH, namely, the thioester and the amide adducts. Interestingly, the disulfide GSSG also reacts with oxanine and forms these two types of adducts. These two types of adducts are shown to form when GSH and GSSG react with oxanine-containing calf thymus DNA as possible DPC derived from cellular proteins. The biological consequences of these two forms of DPC deserve further investigation.

EXPERIMENTAL PROCEDURES

Materials. 2′-Deoxyguanosine, *N*-acetylcysteine (NAc-Cys), N^{α}-acetyllysine (NAc-Lys), N^{α}-acetylarginine (NAc-Arg), *N*-acetyltyrosine (NAc-Tyr) or *N*-acetylserine (NAc-Ser), calf thymus DNA, reduced glutathione (GSH), and oxidized glutathione (GSSG) were purchased from Sigma Chemical Co. (St. Louis, MO). All reagents are of reagent grade or above.

Reversed Phase HPLC Analysis. HPLC chromatography was performed by using a Hitachi L-7000 pump system with a D-7000 interface (Hitachi Ltd., Tokyo, Japan), a Rheodyne injector (Rheodyne, Inc., Cotati, CA), and a L-7450A photodiode array detector (Hitachi Ltd., Tokyo, Japan) for systems 1−3 or a X'TremeSimple nanoflow LC system (Microtech, Orange, CA) for system 4. System 1: A Prodigy ODS (3) column (4.6 × 250 mm, 5 μm (Phenomenex, Torrance, CA)) was eluted with a linear gradient from 100% 50 mM ammonium formate buffer (pH 5.5) to 25% methanol in 50 mM ammonium formate from 0 to 25 min at a flow rate of 1.0 mL/min. System 2: A Prodigy ODS (3) column (4.6 × 250 mm, 5 μm (Phenomenex, Torrance, CA)) was eluted with 100% water in the first 5 min, followed by a linear gradient of 100% water to 80% methanol in water from 5 to 20 min at a flow rate of 1.0 mL/min. System 3: A reversed phase C18 column (Luna, 2.0 × 150 mm, 5 μm (Phenomenex, Torrance, CA)) was eluted with a linear gradient of 100% 10 mM ammonium formate buffer (pH 5.5) to 20% methanol in 10 mM ammonium formate from 0 to 20 min at a flow rate of 0.2 mL/min. After 20 min, the percentage of methanol was increased to 100% in 1 min and maintained at 100% methanol for 5 min before decreasing to 0% methanol and conditioned for 20 min. System 4: A reversed phase C18 column (Bio-Basic 18, 100 mm × 75 μm, 5 μm, 15 μm tip ID (Thermo Electron Corp., Bremen, Germany)) was isocratically eluted at a flow rate of 300 nL/min with 0.1% acetic acid (pH 3.3) for the first 5 min, followed by a linear gradient of 0.1% acetic acid to 10% acetonitrile in 0.1% acetic acid from 5 to 15 min, and the percentage of acetonitrile was increased to 100% in 5 min. The column was washed with 100% acetonitrile for 10 min before conditioning with 0.1% acetic acid for 20 min.

Mass Spectrometry. Mass spectra were recorded on triple quadrupole mass spectrometers: Quattro Ultima (Micromass, Manchester, United Kingdom) equipped with an electrospray ionization (ESI) interface or a TSQ Quantum (Thermo Electron Co., San Jose, CA) equipped with a nanospray ionization (NSI) interface.

NMR Spectrometry. ^{1}H and ^{13}C NMR spectra, including COSY and HMQC correlation, were recorded on a Varian-Unity INOVA-500 MHz NMR spectrometer. Chemical shifts are presented in parts per million from the internal standard tetramethylsilane.

Synthesis of 2′-Deoxyoxanosine (dOxo). 2′-Deoxyoxanosine (dOxo, 5-amino-3-β-(2-deoxy-D-ribofuranosyl)-3*H*-imidazo[4,5-*d*][1,3]oxazin-7-one) was synthesized from a reaction of 2′-deoxyguanosine (1.0 mM) and sodium nitrite (10 mM) in 2 M sodium acetate buffer (pH 3.75) as modified from reported procedures (*7*). The reaction mixture was incubated at 37 °C for 24 h and collected by HPLC using system 1 and desalted by using system 2. The isolated yield of dOxo was 18%. ESI+/MS: *m*/*z* 269 ([dOxo + H]$^{+}$).

Reaction of dOxo with N^{α}-Acetyl α-amino Acids or Glutathione

A solution containing dOxo (0.5 mM), 100 mM N^{α}-acetyl α-amino acid (*N*-acetylcysteine, N^{α}-acetyllysine, N^{α}-acetylarginine, *N*-acetyltyrosine, or *N*-acetylserine) or reduced glutathione (GSH) in the presence of 0.2 M potassium phosphate buffer (pH 7.4 or 8.4) was incubated at 37 °C for 2 h, and the solution pH was adjusted to 5.5 before analysis by HPLC system 1. The product was collected by HPLC using system 1, followed by evaporation and analysis by ESI/MS.

dOxo-NAc-Cys. ESI+/MS: *m*/*z* 432 ([M + H]$^{+}$), 316 ([M + H − 2-deoxyribose]$^{+}$); UVmax: 220, 278 nm (pH 5.5); ^{1}H NMR (D_2O) δ 1.94 (s, 3H, CH_3); 2.49 (m, 1H, 2′-H); 2.57 (m, 1H, 2′-H); 3.24 (dd, *J* = 7.5, 14 Hz, 1H, C*H*$_2$S); 3.60 (dd, *J* = 4.5, 14 Hz, 1H, C*H*$_2$S); 3.67 (dd, *J* = 5.0, 12.5 Hz, 1H, 5′-H); 3.75 (dd, *J* = 3.5, 12.5 Hz, 1 H, 5′-H); 4.02 (m, 1H, 4′-H); 4.46 (dd, *J* = 4.5, 7.5 Hz, 1H, C*H*CH$_2$S); 4.51 (m, 1H, 3′-H); 6.06 (t, *J* = 6.5 Hz, 1H, 1′-H); 7.94 (s, 1H).

dOxo-NAc-Lys. ESI+/MS: *m*/*z* 441 ([M + H]$^{+}$); UVmax: 220, 240 nm (pH 5.5).

dOxo-NAc-Arg. ESI+/MS: *m*/*z* 469 ([M + H]$^{+}$); UVmax: 220, 268 nm (pH 5.5).

dOxo-NAc-Ser. ESI+/MS: *m*/*z* 414 ([M + H]$^{+}$); UVmax: 220, 267 nm (pH 5.5).

dOxo-NAc-Tyr. ESI-/MS: *m*/*z* 490 ([M − H]$^{-}$); UVmax: 220, 254 nm (pH 5.5).

dOxo-S-GSH. ESI-/MS: *m*/*z* 574 ([M − H]$^{-}$); ESI+/MS: *m*/*z* 576 ([M + H]$^{+}$), 460 ([M + H − 2-deoxyribose]$^{+}$); UVmax: 218, 275 nm (pH 5.5); ^{1}H NMR (D_2O) δ 2.11 (dt, *J* = 7.0, 7.0 Hz, 2H, CHC*H*$_2$CH$_2$), 2.46 (t, *J* = 7.0 Hz, 2H, CHCH$_2$C*H*$_2$); 2.53 (m, 1H, 2′-H); 2.61 (m, 1H, 2′-H); 3.34 (dd, *J* = 8.0, 14 Hz, 1H, CH*H*S); 3.62 (dd, *J* = 5.0, 14 Hz, 1H, C*H*HS); 3.70 (dd, *J* = 5.0, 12.5 Hz, 1H, 5′-H); 3.73 (t, *J* = 7.0 Hz, 1H, C*H*CH$_2$CH$_2$); 3.75 (dd, *J* = 3.5, 12.5 Hz, 1 H, 5′-H); 3.79 (s, 2H, NHC*H*$_2$CO$_2$H); 3.82 (m, 1H, 4′-H); 4.07 (m, 1H, 3′-H); 4.71 (dd, *J* = 5.0, 8.0 Hz, 2H, C*H*CH$_2$S); 7.99 (s, 1H, HN−C*H*═N) ppm.; ^{13}C NMR (D_2O) δ 26.2 (CH***C***H$_2$CH$_2$), 29.0(***C***H$_2$S), 31.5 (CHCH$_2$***C***H$_2$), 39.7 (C-2′), 43.5 (NH***C***H$_2$CO$_2$H), 53.1 (***C***HCH$_2$S), 54.2 (***C***HCH$_2$CH$_2$), 61.2 (C-5′), 70.5 (C-3′), 84.2 (C-1′), 87.1 (C-4′), 128.8 (*C*═

C−C(=O)-S), 131.5 (HN-***C***H=N), 134.9 (***C***=C−C(=O)-S), 159.2 (NH-***C***(=O)-NH_2), 171.4, 174.1, 175.0, 176.4 (***C***O_2H and ***C***ONH), 186.4 (***C***(=O)S).

dOxo-N-GSH. ESI+/MS: *m/z* 576 ($[M + H]^+$), 460 ([M + H − 2-deoxyribose]$^+$); UVmax: 213, 240 nm (pH 5.5).

dOxo-N-GSSG. ESI+/MS: *m/z* 880 ($[M + H]^+$), 764 ([M + H − 2-deoxyribose]$^+$); UVmax: 213, 240 nm (pH 5.5).

Acid Hydrolysis of dOxo-S-NAc-Cys. A solution containing dOxo-*S*-NAc-Cys (1.0 mM) in 0.1 N HCl was incubated at 60 °C for 30 min and analyzed by HPLC system 1. Aliquots of the two reaction mixtures were co-injected to HPLC to confirm that they produced the same product by coelution. The product Oxa-*S*-NAc-Cys was collected from HPLC using the same system, evaporated, and analyzed by ESI+/MS.

Oxa-S-NAc-Cys. ESI+/MS: *m/z* 316 ($[M + H]^+$); UVmax: 220, 304 nm (pH 5.5); ^{1}H NMR (D_2O) δ 2.02 (s, 3H, CH_3); 3.37 (dd, J = 8.0, 14 Hz, 1H, CH_2S); 3.66 (dd, J = 4.5, 14 Hz, 1H, CH_2S); 4.66 (dd, J = 8.0, 4.5 Hz, 1H, CHCH_2S); 7.64 (s, 1H).

Acid Hydrolysis of dOxo. 2′-Deoxyoxanosine (5.5 mg) was hydrolyzed in 0.1 N HCl at 37 °C for 2 h to afford 2.6 mg of oxanine in 83% yield.

Stability of Oxa-S-GSH and Oxa-N-GSH under Mild Acid Hydrolysis. A solution containing Oxa-*S*-GSH or Oxa-*N*-GSH (1.0 mM) in 0.1 N HCl was incubated at 60 °C for 30 min or at 37 °C for 2 h and analyzed by HPLC system 1 for recovery.

Stability of Oxa-S-GSH under Alkaline Hydrolysis. A solution containing Oxa-*S*-GSH (1.0 mM) in 0.1 N or 1.0 N NaOH was incubated at 37 °C for 2 h and analyzed by HPLC system 1 to determine the recovery of Oxa-*S*-GSH. In the reaction in 1 N NaOH, an aliquot of the reaction mixture was co-injected with xanthine to confirm the identity of the product.

Reaction of Oxa with GSH or GSSG

A solution containing Oxa (0.5 mM), 100 mM GSH or GSSG in the presence of 0.2 M potassium phosphate buffer (pH 7.4 or 8.4) was incubated at 37 °C for 2 h before analysis by HPLC system 1, monitoring at 268 or 304 nm. The products Oxa-*S*-GSH and Oxa-*N*-GSH were collected from the reaction of Oxa with GSH by HPLC system 1 from 18 to 19 min and 15 to 16 min, respectively, whereas Oxa-*N*-GSSG was collected from 12 to 13 min in the reaction of Oxa with GSSG. The collected fractions were evaporated to dryness, redissolved in water, and collected from HPLC system 2, eluting in water and methanol to remove the salt.

Oxa-S-GSH. (2-Amino-4-[1-(carboxymethyl-carbamoyl)-2-(5-ureido-1*H*-imidazole-4-carbonylsulfanyl)-ethylcarbamoyl]-butyric acid). ESI+/MS: *m/z* 460 ($[M + H]^+$); ESI-/MS: *m/z* 458 ($[M + H]^-$); UVmax: 214, 304 nm (pH 5.5); ϵ_{193} = 11,000 M^{-1} cm^{-1}; ϵ_{304} = 9,350 M^{-1} cm^{-1} (in H_2O); ^{1}H NMR (D_2O) δ 2.14 (dt, J = 7.0, 7.0 Hz, 2H, CHCH_2-CH_2); 2.50 (t, J = 7.0 Hz, 2H, CHCH_2CH_2); 3.33 (dd, J = 8.0, 14 Hz, 1H, CHHS); 3.60 (dd, J = 5.0, 14 Hz, 1H, CHHS); 3.84 (t, J = 7.0 Hz, 1H, CHCH_2CH_2); 3.98 (s, 2H, NHCH_2CO_2H); 4.71 (dd, J = 5.0, 8.0 Hz, 2H, CHCH_2S); 7.66 (s, 1H, HN−CH=N) ppm. ^{13}C NMR (D_2O) δ 28.5 (CH***C***H_2CH_2), 31.3 (***C***H_2S), 33.9 (CHCH_2***C***H_2), 44.0 (NH***C***H_2-CO_2H), *51.5* (***C***H_3OH), 55.9 (***C***HCH_2S), 56.2 (***C***HCH_2CH_2),

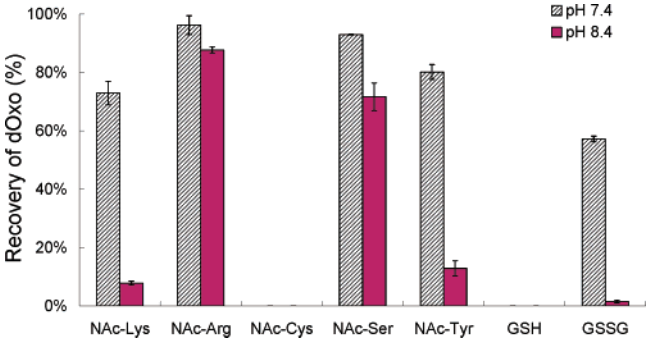

FIGURE 1: Recovery of 2′-dOxo after the reaction with N^{α}-acetylated α-amino acids or peptides at 37 °C at pH 7.4 or 8.4 for 2 h.

121.6 (*C* = ***C***-C(=O)-S), 135.6 (HN-***C***H=N), 138.0 (***C***=C−C(=O)-S), 159.6 (NH-***C***(=O)-NH_2), 174.8, 175.8, 175.9, 177.4 (***C***O_2H and ***C***ONH), 187.4 (***C***(=O)S). The ^{1}H-^{1}H COSY spectrum is shown as Figure S2 in Supporting Information, and the ^{1}H-^{13}C HMQC spectrum is shown as Figure 4 in the text.

Oxa-N-GSSG. (4-[2-[2-(4-Amino-4-carboxy-butyrylamino)-2-(carboxymethyl-carbamoyl)-ethyldisulfanyl]-1-(carboxymethyl-carbamoyl)-ethylcarbamoyl]-2-[(5-ureido-1*H*-imidazole-4-carbonyl)-amino]-butyric acid). The product Oxa-*N*-GSSG was collected from the reaction of Oxa with GSSG by HPLC from 11 to 12 min, evaporated to dryness, redissolved in water, and collected from HPLC system 2 to remove the salt. ESI+/MS: *m/z* 765 ($[M + H]^+$); 383 ($[M + 2H]^{+2}$); UVmax: 214, 268 nm (pH 5.5); ϵ_{272} = 19,200 $M^{-1}cm^{-1}$ (in H_2O); ^{1}H NMR (D_2O) δ 2.1−2.2 (m, 3H, CHCH_2CH_2 and CHCH'H′CH_2), 2.35 (m, 1H, CHCH′H'CH_2), 2.57 (m, 4H, CHCH_2CH_2 and CHCH_2CH'_2); 2.97 (m, 2H, CHHS and CH′H'S); 3.25 (m, 2H, CHHS and CH′H′S); 3.92 (t, 1H, CH'CH_2CH_2); 3.99 (s, 2H, NHCH'_2CO_2H); 4.01 (s, 2H, NHCH_2CO_2H); 4.56 (dd 1H, CHCH_2CH_2), 4.74 (m, 4H, CHCH_2S and CH'CH_2S); 8.27 (s, 1H, HN−CH=N) ppm. ^{13}C NMR (D_2O) δ 26.9, 27.5 (CH***C***H_2CH_2), 32.2, 32.6 (CHCH_2***C***H_2), 39.7, 39.9 (***C***H_2S), 42.3 (NH***C***H_2CO_2H), 53.3 (***C***HCH_2CH_2), 53.5, 53.6 (***C***HCH_2S), 54.3 (***C***HCH_2CH_2), 112.2 (*C*=***C***-C(=O)-N), 132.3 (HN-***C***H=N), 135.3 (***C***=C−C(=O)-N), 158.0 (NH-***C***(=O)-NH_2), 162.2 (C=C-***C***(=O)-N), 173.5, 173.7, 174.0, 174.2, 175.8, 176.2, 176.5 (***C***O_2H and ***C***ONH). The COSY and ^{1}H-^{13}C HMQC spectra are shown in Figure S2 in Supporting Information.

Oxa-N-GSH. (4-[1-(Carboxymethyl-carbamoyl)-2-mercaptoethylcarbamoyl]-2-[(5-ureido-1*H*-imidazole-4-carbonyl)-amino]-butyric acid). Because Oxa-*N*-GSH is the minor product in the reaction of Oxa with GSH, it is obtained in large quantities by the reduction of Oxa-*N*-GSSG using 2 mol equiv of dithiotreitol with vortexing for 2 min. The product Oxa-*N*-GSH was collected from HPLC using system 1 and desalted by collecting from HPLC system 2. After evaporating to dryness, Oxa-*N*-GSH was insoluble in water and was dissolved in 1% trifluoroacetic acid for the following measurements. ESI+/MS: *m/z* 460 ($[M + H]^+$); ESI-/MS: *m/z* 458 ($[M + H]^-$); UVmax: 214, 268 nm (pH 5.5); ϵ_{245} = 7,800; ϵ_{260} = 8,600 $M^{-1}cm^{-1}$ (in 1% trifluoroacetic acid, pH 1.0); ^{1}H NMR (1% CF_3CO_2H in D_2O) δ 2.18 (m, 1H, CHCHHCH_2), 2.36 (m, 1H, CHCHHCH_2), 2.57 (m, 2H, CHCH_2CH_2), 2.93 (t, J = 6.0 Hz, 2H, CH_2S), 4.01 (s, 2H,

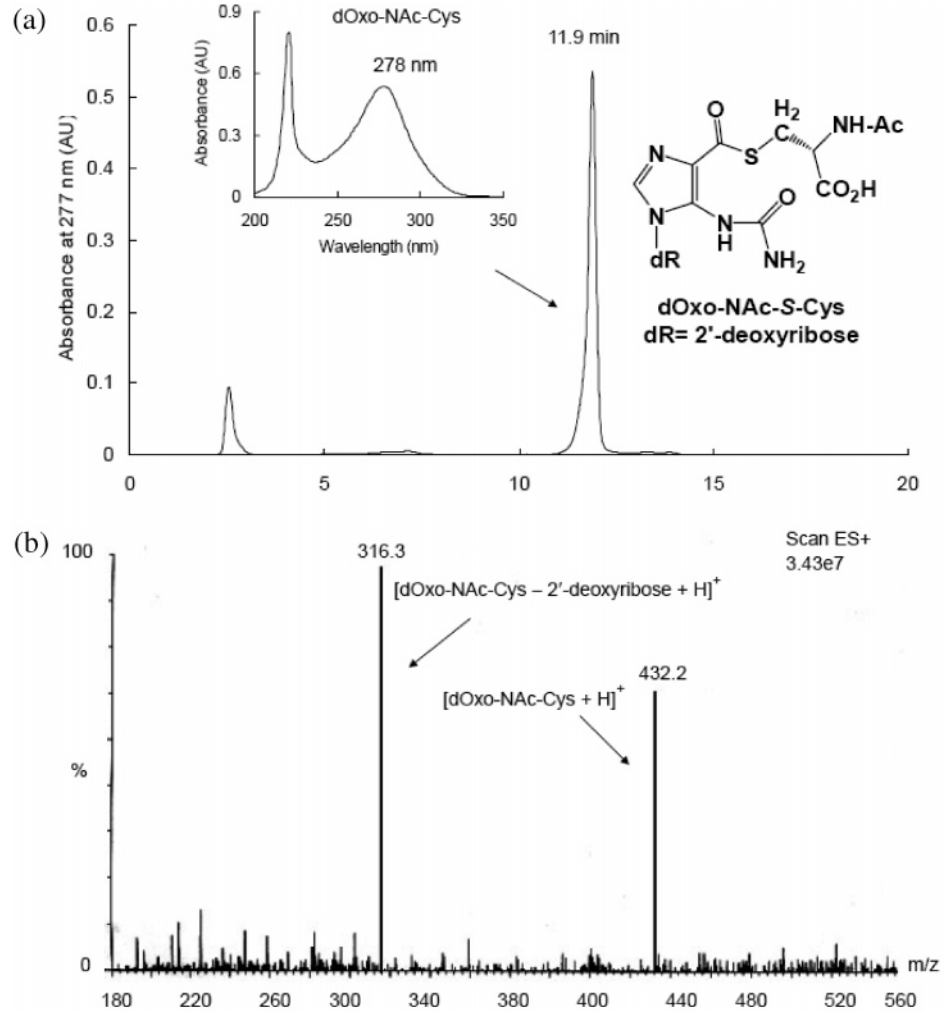

FIGURE 2: HPLC chromatogram of the reaction of 2′-dOxo with NAc-Cys, yielding dOxo-*S*-NAc-Cys.

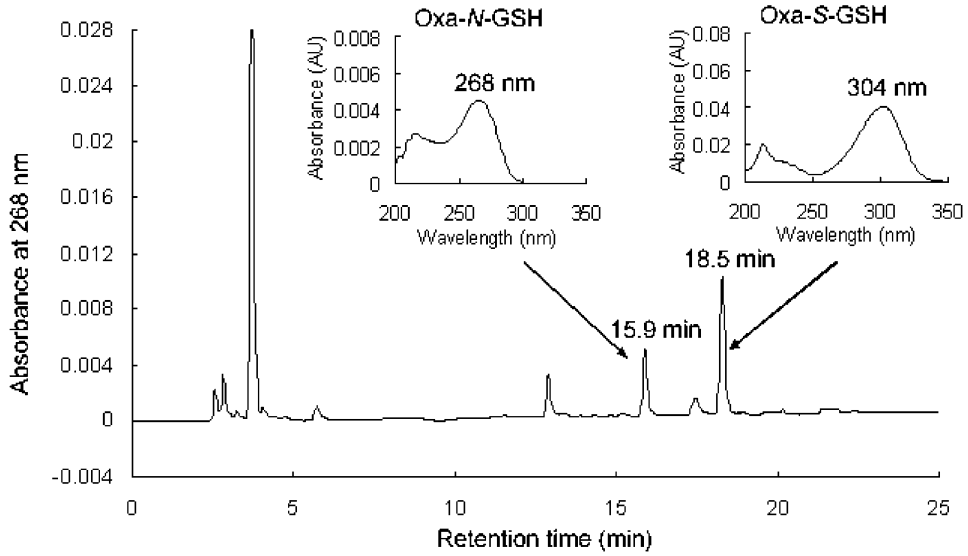

FIGURE 3: HPLC chromatogram of the reaction of oxanine with reduced glutathione (GSH), yielding Oxa-*N*-GSH and Oxa-*S*-GSH.

NHC*H*$_2$CO$_2$H), 4.58 (m, 1H, C*H*CH$_2$S), 4.62 (t, J = 6.0 Hz, 1H, C*H*CH$_2$CH$_2$), 8.62 (s, 1H, HN−C*H*═N) ppm. ^{13}C NMR (1% CF$_3$CO$_2$H in D$_2$O) δ 28.2 (***C***H$_2$S), 29.0 (CH***C***H$_2$CH$_2$), 34.2 (CHCH$_2$***C***H$_2$), 43.7 (NH***C***H$_2$CO$_2$H), 54.8 (***C***HCH$_2$CH$_2$), 58.1 (***C***HCH$_2$S), 112.4 (*C*═***C***-C(═O)-N), *115.4*, *117.8*, *120.1*, *122.4* (***C***F$_3$CO$_2$H), 133.6 (HN-***C***H═N), 136.4 (***C***═C−C(═O)-N), 159.4 (NH-***C***(═O)-NH$_2$), 162.3 (C═C-***C***(═O)-N), *165.1*, *165.4*, *165.6*, *165.9* (CF$_3$***C***O$_2$H), 175.0, 175.6, 177.3, 177.8 (***C***O$_2$H and ***C***ONH). The COSY and ^{1}H-^{13}C HMQC spectra are shown in Figure S3 in Supporting Information.

Time-Dependent Formation of Oxa-S-GSH and Oxa-N-GSH. A solution containing Oxa (1.0 mM) and GSH (5.0 mM) in 100 mM KH$_2$PO$_4$ (pH 7.4, total volume

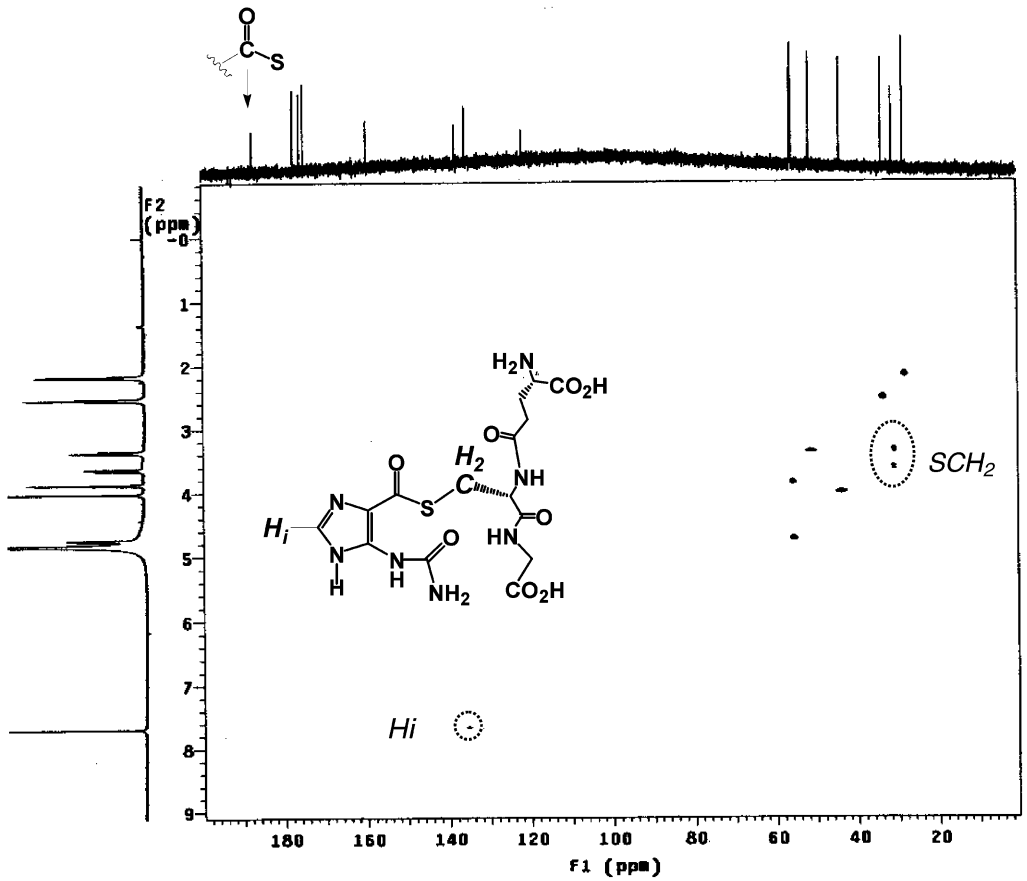

FIGURE 4: ^{1}H-^{13}C heteronuclear multiple quantum coherence (HMQC) spectrum of Oxa-*S*-GSH. The methylene protons of the cysteine residue are in the oval, and the methine proton of the imidazole ring is in the circle.

0.3 mL) was incubated at 37 °C. An aliquot (30 μL) of the solution was removed at 0, 0.25, 0.5, 1.0, 2.0, and 4.0 h and analyzed for the yields of Oxa-*S*-GSH and Oxa-*N*-GSH as well as the recovery of Oxa using HPLC system 1. The experiments were repeated in triplicate.

Synthesis of Oxa-Containing DNA. Oxanine-containing DNA was obtained by incubating a solution containing calf thymus DNA (final concentration of 1.5 mg/mL), sodium nitrite (0.5 M) in 0.2 M sodium acetate buffer (pH 3.7) at 37 °C for 2 h in a final volume of 0.5 mL. The reaction mixture was precipitated with 2 mL of cold ethanol and centrifuged at 22,000*g* at 0 °C for 20 min. The supernatant was removed, and the precipitate was washed twice with 3 mL of 70% cold ethanol and centrifuged at 22,000*g* at 0 °C for 20 min. The precipitate was evaporated and hydrolyzed with 0.5 mL of 0.1 N HCl at 60 °C for 30 min. The pH of the hydrolysate was adjusted to 5.5 before analysis by HPLC system 1 for oxanine content.

HPLC-ESI/MS Analysis of Products from Oxa-Containing DNA with GSH or GSSG. A solution of Oxa-containing calf thymus DNA (final concentration 1.5 mg/mL), GSH, or GSSG (100 mM) in 0.2 M potassium phosphate buffer (pH 7.4 or 8.4) with a final volume of 1.0 mL was incubated at 37 °C for 12 h. The reaction mixture was precipitated, washed, and acid hydrolyzed as described above. The pH of the hydrolysate was adjusted to 5.5 and filtered through a 0.22 μm Nylon syringe filter, and an aliquot (20 μL) was analyzed by HPLC-ESI/MS with a Quattro Ultima (Micromass, Manchester, United Kingdom) equipped with an electrospray ionization (ESI) interface using HPLC system 3. After the MS acquisition was completed, the valve was switched to waste during washing and conditioning before the next run. A voltage of 3.0 kV was applied to the electrospray needle. N_2 was used as the desolvation gas (500 L/h) and as the nebulization gas (150 L/h). The source temperature was at 120 °C, and the stainless steel capillary was heated to 350 °C to obtain optimal desolvation. Argon was used as the collision gas in MS/MS experiments. The pressure of the collision cell was 2.5×10^{-3} mbar. Selective ion monitoring (SIM) was performed at *m*/*z* 460 for Oxa-*S*-GSH and Oxa-*N*-GSH and at *m*/*z* 765 for Oxa-*N*-GSSG.

NanoLC-NSI/MS/MS Analysis of Oxa-S-GSH from HNO_2-Treated DNA with GSH. A solution containing calf thymus DNA (final concentration 1.5 mg/mL) and sodium nitrite (100 or 200 μM) in 0.2 M sodium acetate buffer (pH 3.7) was incubated at 37 °C for 12 h in a final volume of 1.0 mL. The reaction mixture was precipitated, washed, and reconstituted into a solution of Oxa-containing calf thymus DNA (final concentration of 2.0 mg/mL) and incubated with GSH (5 mM) in 0.2 M potassium phosphate buffer (pH 7.4) at 37 °C for 2 h with a final volume of 750 μL. The reaction mixture was precipitated, washed, and acid hydrolyzed as described above. The pH of the hydrolysate was adjusted to 3.3 and enriched by C18-OH SPE as described below. One microliter of the enriched DNA sample, collected after the SPE column described below, was analyzed with HPLC system 4. The column was connected to a TSQ Quantum mass spectrometer (Thermo Electron Co., San Jose, CA) with Xcalibur 1.2 software for data acquisition and analysis (Thermo Electron Co., San Jose, CA) . The mass spectrom-

eter was operated with nanospray ionization in selective reaction monitoring (SRM) mode. The capillary temperature was set at 220 °C and spray voltage at 1.4 kV. A collision energy of 20 V was used with argon at a pressure of 1.5mTorr for collision-induced dissociation (CID). In the SRM experiment, the precursor $[M + H]^+$ ion was generated in the NSI source under the positive ion mode and focused in quadrupole 1 (Q1) and dissociated in a collision cell (quadrupole 2, Q2), yielding the product ion, which was analyzed in quadrupole 3 (Q3). For Oxa-*S*-GSH, the SRM monitored Q1 and Q3 at *m*/*z* 460 and *m*/*z* 296, respectively. Scan time was 0.1 s, and the peak width was 0.3 *m*/*z* for Q1 and 0.7 *m*/*z* for Q3. The yield of Oxa-*S*-GSH was quantified using the calibration curve described below. The experiments were repeated in triplicate.

Enrichment of Oxa-S-GSH by the C18-OH SPE Column. Before use for samples, each batch of SPE columns was tested for consistency in their elution pattern with 5.0 μg each of standard Oxa-*S*-GSH. After elution with the conditions described below, the fractions were collected every 3 mL. The eluant was dried and quantified by HPLC using system 1. The hydrolysate (300 μL) was loaded on a C18-OH SPE column preconditioned with 15 mL of methanol, followed by 15 mL of 0.1% acetic acid (pH 3.3). After the sample was loaded and eluted, the column was washed with 12 mL of 0.1% acetic acid, followed by 3 mL of 10% methanol in 0.1% acetic acid. The fraction containing Oxa-*S*-GSH was eluted with 3 mL of 20% methanol in 0.1% acetic acid in a 4 mL silanized glass vial, evaporated under vacuum with a centrifuge concentrator, and reconstituted in 300 μL of 0.1% acetic acid before nanoLC-NSI/MS/MS analysis.

Calibration Curve. The stock solution of Oxa-*S*-GSH (1.0 mg/mL) in water was stored at −20 °C. The sample solutions for calibration were freshly prepared by diluting the stock solutions in 0.1% acetic acid. Various amounts of Oxa-*S*-GSH ranging from 2.0, 5.0, 10, 20, and 50 fmol/uL were analyzed by nanoLC-NSI/MS/MS in triplicate. The equation of the calibration curves was obtained by linear regression.

RESULTS

Reaction of dOxo with N$^\alpha$-Acetyl α-amino acids. Although 2′-deoxyoxanosine (dOxo) was shown to react with the free amino acid glycine at the *N*-terminal amino group (*16*), the α-amino groups of the amino acid residues in proteins are linked as the amide backbone. Thus, the reaction of dOxo with proteins is most likely to take place at the nucleophilic side chains of the amino acid residues. Incubation of dOxo with individual *N*$^\alpha$-acetylated α-amino acid, such as *N*$^\alpha$-acetylcysteine (NAc-Cys), *N*$^\alpha$-acetyllysine (NAc-Lys), *N*$^\alpha$-acetylarginine (NAc-Arg), *N*$^\alpha$-acetyltyrosine (NAc-Tyr), and *N*$^\alpha$-acetylserine (NAc-Ser), was performed under physiologically relevant conditions. Reversed phase HPLC analysis revealed the formation of a new peak with consumption of dOxo. Electrospray ionization mass spectra of the products suggested the formation of 1:1 addition products of *N*$^\alpha$-acetylated amino acids to dOxo. The reaction of dOxo with the nucleophilic side chains of *N*$^\alpha$-acetylated α-amino acid is expected to open the oxanine ring, breaking the bond between C6 and O1 and forming a new amide linkage. On the basis of the recovery of dOxo, a decreased reactivity was observed in the order NAc-Cys > NAc-Lys > NAc-Tyr > NAc-Ser > NAc-Arg at both pH 7.4 and 8.4 (Figure 1). In the presence of NAc-Cys, dOxo completely disappeared after incubation at 37 °C for 2 h. However, the low reactivity of NAc-Arg and NAc-Ser and the dramatic increase in reactivity of NAc-Lys and NAc-Tyr at pH 8.4 with dOxo are consistent with the nucleophilicity (or the pK_a) of the side chain on these amino acids (*21*).

The reaction of NAc-Cys with dOxo gave a product with a characteristic UV absorption maximum at 214 and 278 nm and a HPLC retention time of 11.9 min (Figure 2a). The positive ESI mass spectrum of this product revealed the protonated molecular ion of the 1:1 adduct of N$^\alpha$Ac-Cys and dOxo at *m*/*z* 432 and the ion with a loss of the 2-deoxyribose (dR) moiety at *m*/*z* 316 (Figure 2b). The reaction of NAc-Lys with dOxo gave a product retaining at 14.9 min on HPLC with UV absorption maxima at 220 and 240 nm. The positive ESI mass spectrum of this product confirmed the formation of an adduct of NAc-Lys with dOxo at *m*/*z* 341. The product of NAc-Tyr with dOxo retained on HPLC at 20.9 min with characteristic UV absorption maxima at 220 and 254 nm and a negative ESI mass spectrum of *m*/*z* 490. Similarly, dOxo reacted with the side chains of NAc-Ser and NAc-Arg to different extents. The HPLC retention times, the characteristic UV absorption, and molecular weights determined by ESI/MS are summarized in Table S1 (Supporting information).

Adducts of Oxa with GSH. In the HPLC chromatogram of oxanine reacting with GSH, two new peaks with distinctly different UV absorption spectra were observed. The early eluting peak showed UV absorption maxima at 220 and 268 nm, whereas the late eluting peak was at 220 and 304 nm (Figure 3). Electrospray ionization mass spectra of the two new peaks eluting at 16 and 18 min in the reaction mixture of oxanine with GSH showed that they both had a molecular weight of 459, suggesting the formation of 1:1 addition products of oxanine and GSH. These two new products should be structural isomers, namely, Oxa-*N*-GSH and Oxa-*S*-GSH, derived from attacking the lactone carbonyl group of oxanine by the amino and thiol groups of GSH to form a new amide and thioester bond, respectively (Scheme 1).

The reaction of oxanine with NAc-Cys yielded a single product with a characteristic UV absorption maximum at 304 nm. It is thus reasonable to postulate that the 18-min peak is the thioester adduct of oxanine and GSH, that is, Oxa-*S*-GSH, whereas the 16-min peak is the amide adduct Oxa-*N*-GSH. The structures of these two adducts are confirmed by their NMR and collision-induced dissociation (CID) mass spectra. In the CID spectrum of GSH, cleavage of the amide bond between γ-glutamate and cysteine gives the b_1 ion at *m*/*z* 130 and the y_2 ion at *m*/*z* 179. However, cleavage of the amide bond between cysteine and glycine yields the b_2 ion at *m*/*z* 233 and the y_1 ion at *m*/*z* 76. The CID mass spectrum of Oxa-*S*-GSH suggests a covalent linkage between cysteine and oxanine moieties based on the b_2' ion at *m*/*z* 385 and the y_2' ions at *m*/*z* 331. Compared to unmodified GSH, in which the b_2 ion is at *m*/*z* 233 and the y_2 ion is at *m*/*z* 179, the difference of 152 mass units between b_2' and b_2 and between y_2' and y_2 indicates that an oxanine moiety is attached to the cysteine residue. However, the CID spectrum of Oxa-*N*-GSH shows b_2' and b_1' ions at *m*/*z* 385 and 282,

Scheme 1: Reaction of Oxa with GSH and GSSG

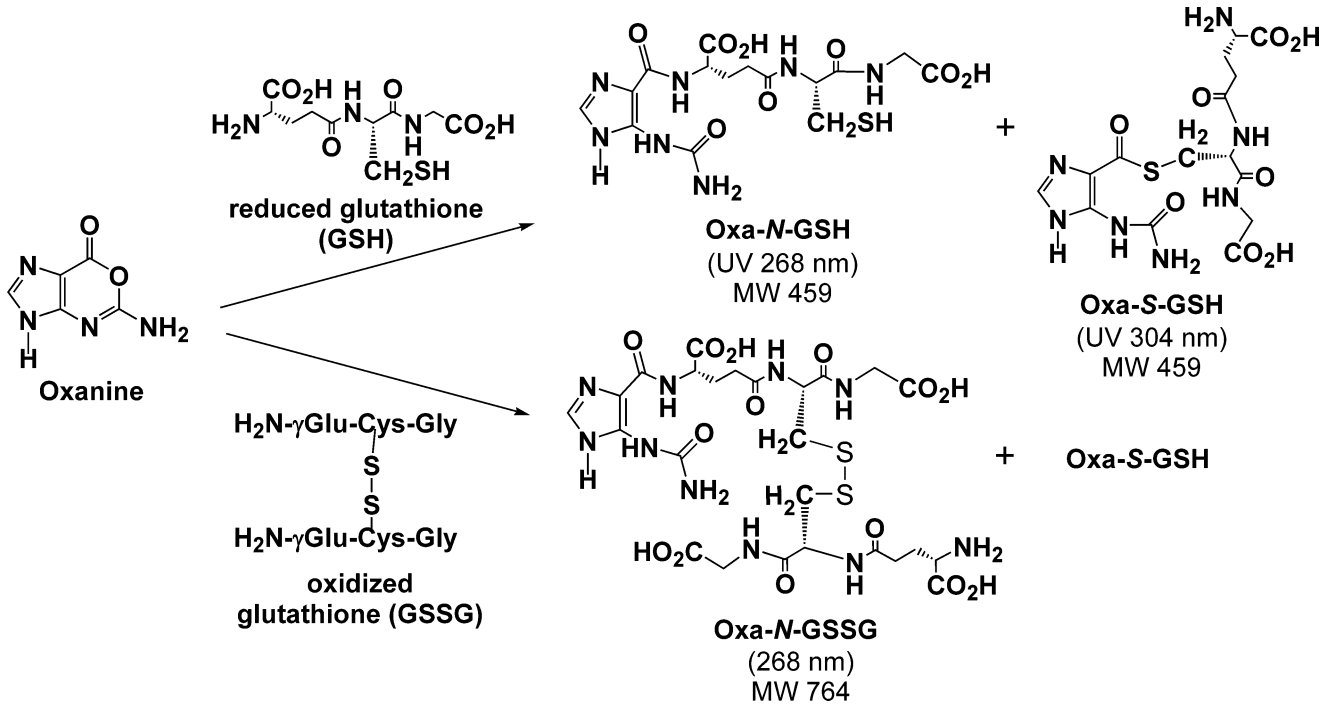

respectively. The difference of 103 mass units between b_2' and b_1' ions of Oxa-*N*-GSH suggests an unmodified cysteine as the second residue. Additionally, the difference of 152 mass units between the b_1' ion of Oxa-*N*-GSH and the b_1 ion from GSH confirmed that oxanine is connected to the γ-glutamate residue (Table 1, summarized from the spectra in Figure S4, Supporting Information).

The ^{1}H NMR spectrum of Oxa-*S*-GSH shows a big downfield shift of 0.52 ppm for the methylene protons of the cysteine residue at a chemical shift of 3.33 ppm compared to that of 2.81 ppm in GSH. A downfield shift of 0.28 ppm for the methine proton of of the cysteine residue in Oxa-*S*-GSH (4.71 ppm) relative to that of GSH (4.43 ppm) is also observed (Table 2). As suggested by the ^{1}H-^{13}C heteronuclear multiple quantum coherence (HMQC) spectrum of Oxa-*S*-GSH, the methylene protons in the cysteine residue split 0.27 ppm apart (at 3.33 and 3.60 ppm) as two sets of doublets of doublets on the carbon at 31.3 ppm (Figure 4, oval). This splitting of the methylene protons in the cysteine residue was also observed with Oxa-*S*-NAc-Cys, dOxo-*S*-NAc-Cys, and dOxo-*S*-GSH (Table 2), presumably due to the formation of a rigid conformation through intramolecular H-bondings with the ureidyl group at C-5 of the imidazole ring. The methine proton on the imidazole ring at 7.66 ppm has a cross-peak with the carbon at 135.6 ppm (circle).

In the ^{1}H NMR spectrum of Oxa-*N*-GSH, the fact that the methine proton in the glutamate residue shifts downfield for ca. 0.93 ppm, from 3.69 ppm in GSH to 4.62 ppm, and that its neighboring methylene protons split 0.18 ppm apart (2.18 and 2.36 ppm) suggests a connection between the γ-glutamate amino group in the GSH moiety and oxanine. In contrast, the chemical shift of the methylene protons of the cysteine residue (2.93 ppm) in Oxa-*N*-GSH is similar to that in GSH (2.81 ppm), and their patterns are triplet in both Oxa-*N*-GSH and GSH (Table 3), strongly suggesting that the cysteine residue is not linked to oxanine.

Furthermore, the signals of 187 and 186 ppm in the ^{13}C NMR spectrum of Oxa-*S*-GSH (Figure 4) and dOxo-*S*-GSH, respectively, provide convincing evidence for their being thioesters. However, the chemical shift of the amide carbon connected to the imidazole moiety is much lower than that of the thioester, for example, 162 ppm in both the dOxo-glycine adduct (*16*) and in Oxa-*N*-GSH (Table 3).

Adducts of Oxa with GSSG. In the HPLC chromatogram of the reaction of oxanine with GSSG, two new peaks eluted at 12 and 18 min (Figure 5a). The 12-min peak is the major product, and it absorbs UV at 268 nm with a molecular weight of 764 according to ESI/MS. Together with an increase of 152 mass units compared to that of GSSG, it is suggested to be the 1:1 adduct of oxanine and GSSG with an amide linkage, Oxa-*N*-GSSG. The CID spectrum of Oxa-*N*-GSSG with an ion at *m*/*z* 690 corresponding to the b_2'-γECG ion, a γE^{oxa}CG-y_2 ion at *m*/*z* 636, and a large b_2'-y_2-NH_3 ion at *m*/*z* 544 provides strong evidence that oxanine is covalently bonded to the γ-glutamate residue (Table 1, summarized from the spectra in Figure S5, Supporting Information). Treatment of Oxa-*N*-GSSG with dithiotreitol reduced the disulfide to yield Oxa-*N*-GSH, the 18-min peak in the reaction of Oxa with GSH as shown in Figure 3. The similar UV absorption at 268 nm for Oxa-*N*-GSSG and Oxa-*N*-GSH indicates that they are structurally related. It was surprising to observe Oxa-*S*-GSH as a minor product in the reaction of oxanine with GSSG. Its identity was confirmed on the basis of its UV absorption at 304 nm, the molecular weight of 459, and coelution in HPLC with Oxa-*S*-GSH isolated from the reaction mixture of Oxa with GSH (Figure 5b). The possibility of GSSG being transformed into GSH during the reaction was excluded because an analysis of a GSSG solution incubated under the same conditions by HPLC-UV and mass spectrometry did not indicate conversion of GSSG to GSH. We thus postulate that the sulfur atom in the disulfide bridge of GSSG initially attacks the lactone

Table 1: Assignment of Collision-Induced Dissociation Mass Spectra of GSH, Oxa-*S*-GSH, Oxa-*N*-GSH, GSSG, and Oxa-*N*-GSH under Positive Electrospray Ionization

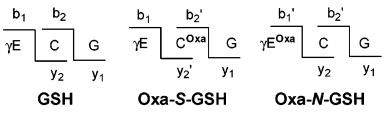

mass detected	assignment
GSH	
75.7	y_1
129.7	b_1
178.9	y_2
214.9	$b_2 - H_2O$
232.8	b_2
307.8	$[M + H]^+$
Oxa-*S*-GSH	
152.6	$[Oxa + H]^+$
296.2	$y_2' - H_2O - NH_3$
312.9	$y_2' - H_2O$
331.3	y_2'
368.1	$b_2' - NH_3$
385.0	b_2'
443.2	$[M' - NH_3 + H]^+$
460.2	$[M' + H]^+$
Oxa-*N*-GSH	
75.8	y_1
152.8	$[Oxa + H]^+$
178.7	y_2
264.8	$b_1' - NH_3$
282.2	b_1'
350.3	$b_2' - NH_3 - H_2O$
367.9	$b_2' - NH_3$
385.0	b_2'
443.0	$[M' - NH_3 + H]^+$
460.2	$[M' + H]^+$

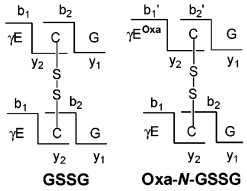

mass detected	assignment
GSSG	
130.1	b_1
354.9	y_2-y_2
391.8	b_2-$y_2 - NH_3$
408.9	b_2-y_2
484.2	γECG-y_2
537.9	b_2-γECG
613.3	$[M' + H]^+$
Oxa-*N*-GSSG	
152.8	$[Oxa + H]^+$
355.1	y_2-y_2
484.1	γECG-y_2
544.2	b_2'-$y_2 - NH_3$
636.3	$\gamma E^{oxa}CG$-y_2
673.3	b_2'-γECG − NH_3
690.5	b_2'-γECG
765.3	$[M' + H]^+$

carbonyl of oxanine and that the disulfide bond is subsequently cleaved to yield Oxa-*S*-GSH.

In the ^{1}H NMR spectrum of Oxa-*N*-GSSG, the methylene protons of the two glutamate residues are two sets of multiplets from 2.1 to 2.4 ppm, suggesting the neighboring effect of the ureidyl group on the imidazole. The methine protons of the two glutamate residues have very different chemical shifts: one at 3.92 ppm as a triplet and the other one at 4.55 ppm as a multiplet. The former is the glutamate residue not connected to oxanine because its pattern and chemical shift are close to those of GSH (triplet, 3.69 ppm) and Oxa-*S*-GSH (triplet, 3.84 ppm) in which the glutamate residue is not connected to oxanine. However, the 4.55 ppm multiplet is assigned as the glutamate residue connected to oxanine because of the large downfield shift and the splitting pattern of doublet of doublet. There are two singlet peaks for the methylene protons in the two glycine residues (Table 2). In the ^{13}C NMR spectrum of Oxa-*N*-GSSG, nearly all of the carbon signals for the glutamate and cysteine residues of GSSG spited into two sets, confirming two different environments for the two glutamate, cysteine, and glycine residues in the molecule. In addition, the newly formed amide bond has a chemical shift of 162 ppm, same as those of Oxa-*N*-GSH and the dO-glycine adduct reported (*16*) (Table 3).

Stability of Oxa-S-GSH and Oxa-N-GSH. It is expected that the thioester adduct Oxa-*S*-GSH is more labile than the amide adduct Oxa-*N*-GSH because it is a thioester in nature. Both Oxa-*S*-GSH and Oxa-*N*-GSH were stable, with quantitative recovery, in the presence of 0.1 N HCl or 0.1 N NaOH at 37 °C for 2 h or in 0.1 N HCl at 60 °C for 30 min. Hydrolysis of Oxa-*S*-GSH is expected to release GSH and form 5-ureido-1*H*-imidazole-4-carboxylic acid. However, when Oxa-*S*-GSH was incubated in 1 N NaOH at 37 °C for 2 h, xanthine was obtained, as confirmed by its negative ESI mass spectrum showing the $[M - H]^-$ ion at *m*/*z* 151 and

Table 2: ^{1}H NMR Chemical Shifts of 2′-Deoxyoxanosine and Oxanine Adducts

^{1}H NMR	GSH[a]	dOxo-*S*-GSH[a]	dOxo-*S*-NAc-Cys[a]	Oxa-*S*-NAc-Cys[a]	Oxa-*S*-GSH[a]	Oxa-*N*-GSSG[a]	Oxa-*N*-GSH[b]
CHC***H***$_2$CH$_2$	2.03 (q)	2.14 (dt)			2.14 (dt)	2.20−2.22 (m) 2.34 (m)	2.18 (dt) 2.36 (dt)
CHCH$_2$C***H***$_2$	2.42 (t)	2.50 (t)			2.50 (t)	2.55−2.60 (m)	2.57 (m)
C***H***CH$_2$CH$_2$	3.69 (t)	3.84 (t)			3.84 (t)	3.92 (t) 4.55 (dd)	4.62 (t)
C***H***$_2$S	2.81 (t)	3.34 (dd) 3.62 (dd)	3.24 (dd) 3.60 (dd)	3.37 (dd) 3.66 (dd)	3.33 (dd) 3.60 (dd)	3.25 (dd) 2.97 (dd)	2.93 (t)
C***H***CH$_2$S	4.43(t)	4.71 (dd)	4.46 (dd)	4.66(dd)	4.71 (dd)	4.74 (m)	4.58 (t)
NHC***H***$_2$CO$_2$H	3.84 (s)	3.79 (s)			3.98 (s)	3.99 (s) 4.01 (s)	4.01 (s)
HNC***H***═N		7.99 (s)	7.94 (s)	7.64 (s)	7.66 (s)	8.27 (s)	8.62 (s)
1′-H		6.12 (t)	6.06 (t)				
2′-H		2.49−2.56 (m)	2.49 (m)				
2″-H		2.57−2.65 (m)	2.57 (m)				
3′-H		4.06−4.07 (m)	4.51 (m)				
4′-H		3.81−3.83 (m)	4.02 (m)				
5′-H		3.70 (dd)	3.67 (dd)				
5″-H		3.75 (dd)	3.75 (dd)				
CH$_3$			1.94 (s)	2.02 (s)			

[a] Measured in D_2O. [b] Measured in 1% trifluroacetic acid in D_2O.

Table 3: ^{13}C NMR Chemical Shifts of 2′-Deoxyoxanosine and Oxanine Adducts

^{13}C NMR	dOxo-*N*-glycine[a]	dOxo-*S*-GSH[b]	Oxa-*S*-GSH[b]	Oxa-*N*-GSSG[b]	Oxa-*N*-GSH[c]
CH***C***H$_2$CH$_2$		26.2	28.5	26.9, 27.4	29.0
CHCH$_2$***C***H$_2$		31.5	33.9	32.2, 32.6	34.2
CHCH$_2$CH$_2$		54.2	56.2	53.3, 54.3	54.8
CH$_2$S		29.0	31.3	39.7, 39.9	28.2
CHCH$_2$S		53.1	55.9	53.5, 53.6	58.1
NH***C***H$_2$CO$_2$H	41.9	43.5	44.0	42.3	43.7
C═C−C(═O)-S		134.9	138.0		
C═***C***−C(═O)-S		128.8	121.6		
C═C−C(═O)-N	131.6			135.3	136.4
C═***C***−C(═O)-N	123.9			112.2	112.4
HN−***C***H═N	130.4	131.5	135.6	132.3	133.6
NH−***C***(═O)-NH$_2$	156.6	159.2	159.6	158.9	159.4
C O$_2$H and ***C*** ONH	171.5 (CO_2H)	171.4, 174.1 175.0, 176.4	174.8, 175.8 175.9, 177.4	173.5, 173.7, 174.0, 174.2 175.8, 176.2, 176.5	175.0, 175.6 177.3, 177.8
C═C−***C***(═O)-S		186.4	187.4		
C═C−***C***(═O)−N	162.1			162.2	162.3
C-1′	84.2	84.2			
C-2′	30.9	39.7			
C-3′	70.5	70.5			
C-4′	87.6	87.1			
C-5′	61.5	61.2			

[a] Measured in DMSO-d_6 as adapted from ref 16 (*16*). [b] Measured in D_2O. [c] Measured in 1% trifluroacetic acid in D_2O.

by co-injection with an authentic standard (data not shown). The mechanism might involve the initial ring opening (lactone hydrolysis) to form 5-ureido-1*H*-imidazole-4-carboxylic acid, which subsequently underwent ring closure to give xanthine, as was observed for the conversion of oxanosine to xanthosine in alkaline conditions (*22*). In contrast, Oxa-*N*-GSH was kept intact under these conditions.

Time-Dependent Formation of Oxa-S-GSH and Oxa-N-GSH. To investigate the rates of Oxa-*S*-GSH and Oxa-*N*-GSH formation, the reaction between oxanine and GSH at 37 °C at pH 7.4 was monitored at various time points from 0 to 4 h using HPLC-UV. The yields of Oxa-*S*-GSH and Oxa-*N*-GSH as well as the recovery of Oxa were measured (Figure 6). A rapid increase in the yield of Oxa-*S*-GSH was observed for up to 1 h, whereas Oxa-*N*-GSH was detectable after incubation for 2 h. The big difference in their yields was consistent with a much greater reactivity for NAc-Cys toward dOxo compared to that of NAc-Lys shown in Figure 1. The time-dependent formation of Oxa-*S*-GSH was in accord with the consumption of Oxa, which was present at 12% after 4 h. This result suggests that oxanine has a lifetime that is long enough to react with GSH before its decomposition.

Reaction of Oxa-Containing DNA with GSH and GSSG. The thioester and the amide adducts were also formed when GSH or GSSG (100 mM) reacted with Oxa-containing calf thymus DNA. A solution of calf thymus DNA was incubated with 0.5 M of HNO_2 at 37 °C for 2 h, followed by precipitation and washing to remove excess HNO_2. The HPLC-UV analysis revealed the formation of 3.0% of oxanine in this DNA sample after mild acid hydrolysis (0.1 N HCl at 60 °C for 30 min). This Oxa-containing DNA solution was incubated with 100 mM GSH at 37 °C (pH 7.4) for 12 h, followed by precipitation and washing to remove excess GSH. An analysis of the DNA acid hydrolysate by HPLC-ESI/MS revealed the formation of Oxa-*S*-GSH as the major product and Oxa-*N*-GSH as the minor product. Figure 7a showed that Oxa-*N*-GSH eluted at 16.7 min and

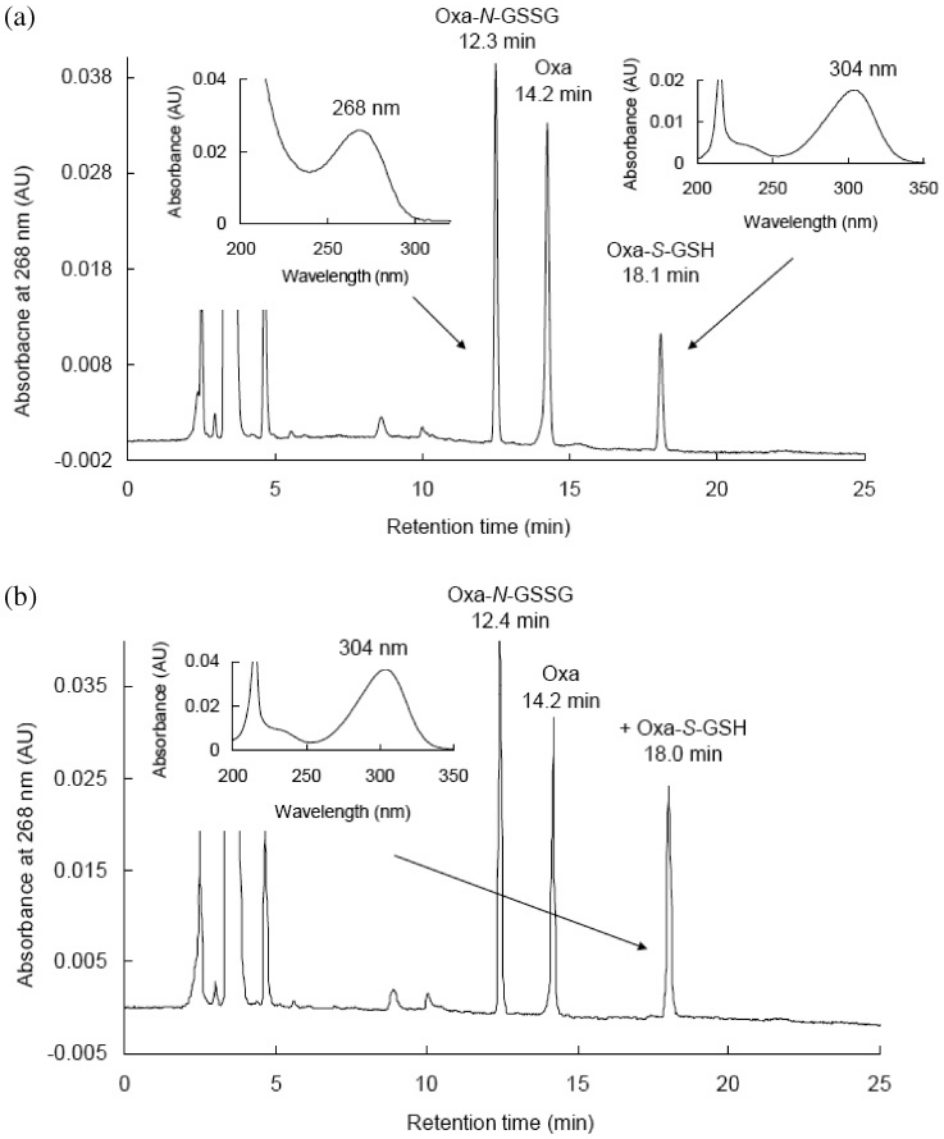

FIGURE 5: (a) HPLC chromatogram of oxanine reacting with oxidized glutathione (GSSG) at 37 °C for 2 h at pH 7.4, producing Oxa-*N*-GSSG and Oxa-*S*-GSH. (b) Co-injection of the reaction mixture with synthetic Oxa-*S*-GSH (0.39 μg).

Oxa-*S*-GSH eluted at 17.9 min under the selective ion monitoring mode at *m*/*z* 460. Their identity was confirmed by comparing the retention times with those of standard Oxa-*N*-GSH and Oxa-*S*-GSH and by their daughter ion spectra (not shown).

Incubation of Oxa-containing DNA with GSSG under the same conditions generated Oxa-*N*-GSSG as the major product and Oxa-*S*-GSH as the minor product as shown by the overlaid LC/MS chromatogram of Oxa-*N*-GSSG at *m*/*z* 765 and Oxa-*S*-GSH at *m*/*z* 460 (Figure 7b). These results suggest that the chemistry of Oxa-containing DNA with GSH and GSSG is similar to that of Oxa itself.

When the concentrations of nitrite and GSH were reduced to physiologically relevant concentrations, that is, 100−200 μM and 5 mM, respectively, Oxa-*S*-GSH, but not Oxa-*N*-GSH, was detected by a highly sensitive nanoLC-NSI/MS/MS assay monitoring at *m*/*z* 460 → 296. Using a calibration curve (R^2 = 0.9993, Figure S6, Supporting Information), the yield of Oxa-*S*-GSH was determined to be 0.0015% with 100 μM nitrite and 0.0018% with 200 μM nitrite (Figure 8).

DISCUSSION

Oxanine in DNA, induced by NO and HNO_2, is reactive toward biological nucleophiles, and it could cross-link with amino acids, peptides, proteins, or other biomolecules. To characterize the chemical structures of oxanine-induced DPCs and to elucidate the mechanism of DPCs formation, we used GSH as a model protein in this study because it contains a thiol and an amino group, the two most reactive nucleophilic side chains of amino acids. Glutathione is the major thiol antioxidant present at high concentration in the cytosol (1−11 mM), nuclei (3−15 mM), and mitochondria (5−11 mM) (*23*−*25*). Nitric oxide is produced in mitochondria as a regulator of mitochondrial functions (*26*−*28*). Moreover, studies showed that mitochondrial DNA might be more prone to nitrosative damage than nuclear DNA because of the rich radical production in the respiratory chain, the lack of protection by histone proteins, and the relatively inefficient DNA repair system (*29*−*32*). Although the levels of oxidative damage in mitochondrial and nuclear DNA are debatable because of analytical methods (*33*), mitochondrial DNA might be an important target for nitrosative damage, and it

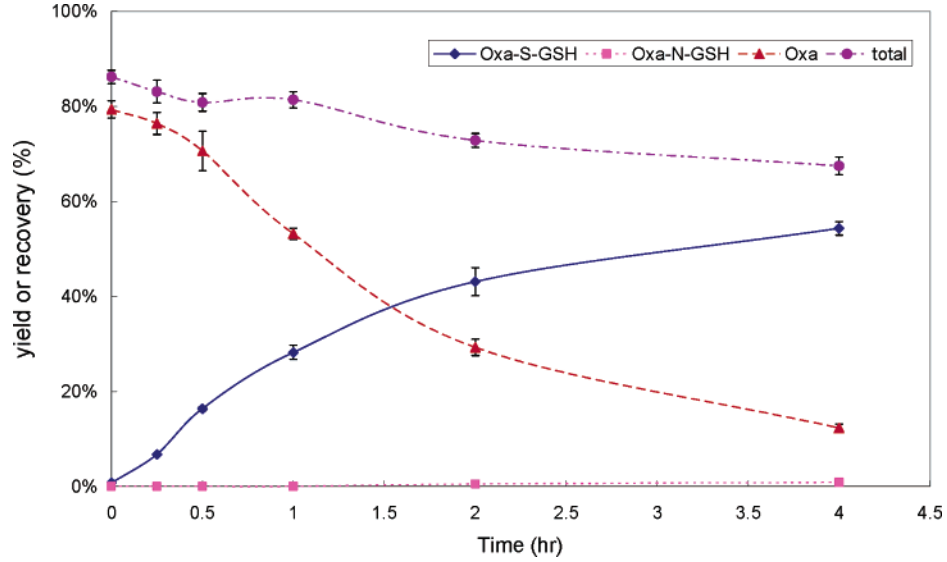

FIGURE 6: Time-dependent formation of Oxa-*S*-GSH and Oxa-*N*-GSH. A solution containing Oxa (1.0 mM) and GSH (5.0 mM) in 100 mM KH_2PO_4 (pH 7.4) was incubated at 37 °C, and the reaction was monitored by analyzing with HPLC-UV at various time points as described in Experimental Procedures. The data points represent the means of triplicate determinations.

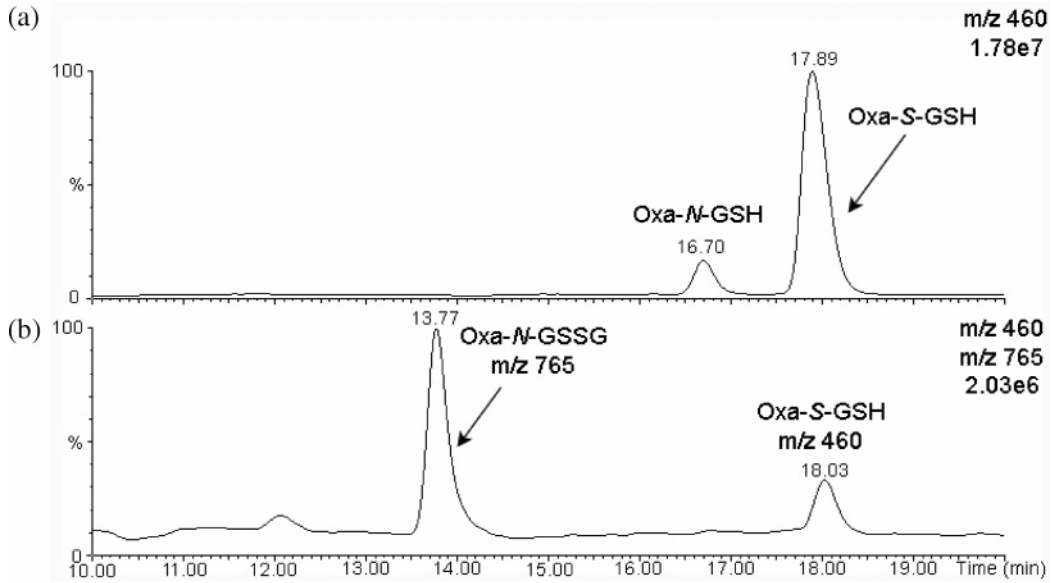

FIGURE 7: HPLC/MS chromatogram of oxanine-containing calf thymus DNA reacting with (a) GSH or (b) oxidized glutathione (GSSG) at 37 °C for 12 h at pH 7.4, followed by acid hydrolysis with 0.1 N HCl at 60 °C for 30 min. Selected ion monitoring at *m*/*z* 460 was performed in the upper panel, whereas the lower panel shows the overlaid chromatogram monitoring at *m*/*z* 460 and *m*/*z* 765.

plays an imperative role in cancer development (*34*, *35*). The reaction of GSH with oxanine in DNA may prevent protein damage. Under high oxidative stress conditions in which GSH is depleted, the oxanine-derived thioester and amide adducts might be important forms of DPCs of cellular proteins.

Our results demonstrate the generation of a novel thioester adduct preferably produced from oxanine with the thiol group of GSH in addition to the amide form of the oxanine-amine adduct. To the best of our knowledge, this is the first article on the characterization of a thioester DPC formed between oxanine and a thiol. The thioester is also detected in the oxanine reaction with the disulfide GSSG as a minor adduct. Both the thioester and amide adducts of oxanine represent two possible forms of DPCs, which can be derived from the side chains of cysteine, lysine, the disulfide bridge of cystine, and the N-terminal of a protein. The reactivity of oxanine with glutathione and DNA-binding proteins might contribute to the reported cytotoxicity and antibacterial activity of oxanosine (*36*, *37*).

It has been shown that the glycosidic linkage of dOxo is as stable as that of dGuo in oligonucleotides (*14*). However, the half-life of the nucleoside dOxo was determined to be 350 h and that for the dOxo-Gly amide adduct is longer, being 1280 h (*16*), suggesting that the amide form of oxanine-derived DPC is a relatively long-lived cellular lesion that can cause detrimental effects if not efficiently repaired. Both the thioester and the amide forms of DPCs are stable under mild acid hydrolysis conditions, which enable their analysis by LC/ESI/MS. Attempts to perform hydrolysis with nucleases failed because of the insolubility of Oxa-containing DNA cross-linked to GSH in buffers at neutral pH. Hydrolysis of the DPCs with mild acid led to the cleavage of the glycosidic bond between the cross-linked oxanine moiety

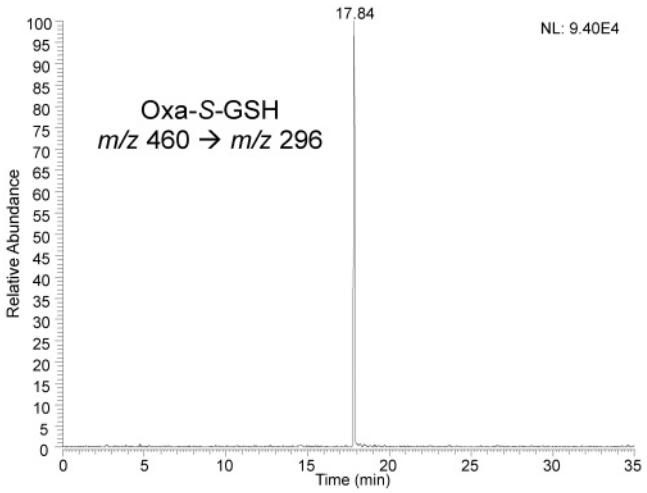

FIGURE 8: HPLC/MS/MS chromatogram of the acid hydrolysate of calf thymus DNA incubated with HNO_2 (200 μM) at 37 °C for 12 h, followed by a reaction with GSH (5 mM) at 37 °C for 2 h at pH 7.4. Selected reaction monitoring at *m*/*z* 460 → 296 was performed for the Oxa-*S*-GSH analysis.

and the 2-deoxyribose (dR) of DNA but left the peptide bonds intact. The mass spectrometric analysis of the resulting peptides modified by oxanine is very useful in the identification of the reaction site by comparing the CID spectra with that of the unmodified peptide. However, most of the mass spectra of amino acids or peptides cross-linked with the nucleoside dOxo contain a $[M - dR]^-$ fragment ion, and the interpretation of the DPC structures of peptides or proteins with dOxo from their mass spectra would be more complicated than those with oxanine. Characterization of the oxanine-derived thioester and amide forms of DPCs by LC/ESI/MS analysis sheds light on the detection of DPCs in cellular DNA. Nakano et al. showed that oxanine binds to DNA-binding proteins, including DNA glycosylases, histone, and high mobility group protein (*15*). But the sites of these proteins cross-linked to oxanine were not determined. Thus, the LC/ESI/MS analysis will be a very helpful tool in the characterization of these DPC structures. Furthermore, oxanine-induced DPC formation is at a much faster rate with DNA glycosylases than with the other two types of proteins (*15*), suggesting a possible role of oxanine in inhibiting DNA base excision repair (BER) enzymes.

Oxanine on DNA was shown to be repaired by human alkyladenine glycosylase (*17*), *Escherichia coli* 3-methyladenine DNA glycosylase II (AlkA), and Endo VIII, but the repair activities of the latter two enzymes on oxanine were much lower than that on xanthine (*18*). Although excision activity for oxanine was observed with bacterial endonuclease V (*19*), oxanine was poorly processed by human DNA glycosylases and HeLa cell-free extracts (*20*). Nonetheless, the prokaryotic UvrABC nuclease and human nucleotide excision repair (NER) enzymes efficiently excised cross-links of spermine, a polyamine, with oxanine-containing oligonucleotides as a model DPC (*20*). The DPCs of oxanine-containing DNA with proteins are much more bulky than this model cross-link of oxanine with spermine. To decipher the complicated biological consequences of cellular DPCs derived from oxanine, the questions concerning whether the bulky the DPCs can be effectively repaired by the NER enzymes and/or whether the NER enzymes preferentially cross-link to oxanine need to be answered. If not repaired, the bulky covalent DPCs result in DNA helix distortion and have the potential to cause mutagenic and cytotoxic effects (*38*−*42*).

Reactive nitrogen oxides species are interconvertible. Nitric oxide is metabolized *in vivo* to nitrite, whereas acidified nitrite can be reduced to nitric oxide by ascorbate in the stomach (*43*−*46*) and by ascorbic acid and quercetin in the saliva (*47*). Exposure to excess nitrite from the diet or overproduction of nitric oxide at sites of chronic inflammation may play an important role in stomach cancer (*48*, *49*). In the presence of oxygen, NO is converted to nitrous anhydride (N_2O_3), a principal nitrosating agent, which is hydrolyzed to nitrite (*50*). Nitric oxide combines with a superoxide anion to form the powerful nitrating agent peroxynitrite at a diffusion-controlled rate (*51*, *52*). In addition to its endogenous origin, NO is also a constituent of cigarette smoke and an air pollutant (*53*). Thus, the formation of oxanine-derived DPCs can be a result of environmental exposure to NO as well as reactive nitrogen oxides species produced *in vivo*.

Dong et al. reported that the base deamination products were formed as major products, whereas dOxo was below the limit of detection when isolated DNA or cells was exposed to physiological concentrations of nitric oxide and oxygen at neutral pH (*54*, *55*). Nonetheless, oxanine, if formed in the cellular systems, is reactive toward nucleophiles, whereas the deamination products are not. It is possible that oxanine reacts with nucleophiles before or during DNA isolation and enzyme digestion processes. Future studies in the detection and identification of the thioester and amide adducts of oxanine with GSH and cellular proteins *in vivo* will confirm the role of oxanine as an intermediate of cellular damage derived from NO and HNO_2.

Because DPC is a type of cellular damage that might be difficult to repair, characterization of the thioester and the amide forms of DPCs derived from oxanine and glutathione should shed light on the mechanism of DPCs formation, their detection *in vivo*, and their biological significance.

ACKNOWLEDGMENT

We thank Professor Pi-Tai Chou (National Taiwan University) for helpful discussions.

SUPPORTING INFORMATION AVAILABLE

HPLC retention times, characteristic UV absorbance maxima, and molecular weights of 2′-deoxyoxanosine and oxanine adducts, and literature data of dOxo-glycine. This material is available free of charge via the Internet at http://pubs.acs.org.

REFERENCES

1. Ohshima, H., and Bartsch, H. (1994) Chronic infections and inflammatory processes as cancer risk factors: possible role of nitric oxide in carcinogenesis, *Mutat. Res. 305*, 253−264.
2. Wink, D. A., Vodovotz, Y., Laval, J., Laval, F., Dewhirst, M. W., and Mitchell, J. B. (1998) The multifaceted roles of nitric oxide in cancer, *Carcinogenesis 19*, 711−721.
3. Wink, D. A., Kasprzak, K. S., Maragos, C. M., Elespuru, R. K., Misra, M., Dunams, T. M., Cebula, T. A., Koch, W. H., Andrews, A. W., Allen, J. S., and Keefer, L. K. (1991) DNA deaminating ability and genotoxicity of nitric oxide and its progenitors, *Science 254*, 1001−1003.

4. Nguyen, T., Brunson, D., Crespi, C. L., Penman, B. W., Wishnok, J. S., and Tannenbaum, S. R. (1992) DNA damage and mutation in human cells exposed to nitric oxide in vitro, *Proc. Natl. Acad. Sci. U.S.A. 89*, 3030−3034.
5. deRojas-Walker, T., Tamir, S., Ji, H., Wishnok, J. S., and Tannenbaum, S. R. (1995) Nitric oxide induces oxidative damage in addition to deamination in macrophage DNA, *Chem. Res. Toxicol. 8*, 473−477.
6. Tamir, S., Burney, S., and Tannenbaum, S. R. (1996) DNA damage by nitric oxide, *Chem. Res. Toxicol. 9*, 821−827.
7. Suzuki, T., Yamaoka, R., Nishi, M., Ide, H., and Makino, K. (1996) Isolation and characterization of a novel product, 2′-deoxyoxanosine, from 2′-deoxyguanosine, oligodeoxynucleotide, and calf thymus DNA treated by nitrous acid and nitric oxide, *J. Am. Chem. Soc. 118*, 2515−2516.
8. Kono, Y., Shibata, H., Adachi, K., and Tanaka, K. (1994) Lactate-dependent killing of *Escherichia coli* by nitrite plus hydrogen-peroxide: A possible role of nitrogen dioxide, *Arch. Biochem. Biophys. 311*, 153−159.
9. Klebanoff, S. J. (1993) Reactive nitrogen intermediates and antimicrobial activity: role of nitrite, *Free Radical Biol. Med. 14*, 351−360.
10. Suzuki, T., Ide, H., Yamada, M., Endo, N., Kanaori, K., Tajima, K., Morii, T., and Makino, K. (2000) Formation of 2′-deoxyoxanosine from 2′-deoxyguanosine and nitrous acid: mechanism and intermediates, *Nucleic Acids Res. 28*, 544−551.
11. Lucas, L. T., Gatehouse, D., and Shuker, D. E. (1999) Efficient nitroso group transfer from *N*-nitrosoindoles to nucleotides and 2′-deoxyguanosine at physiological pH. A new pathway for N-nitrosocompounds to exert genotoxicity, *J. Biol. Chem. 274*, 18319−18326.
12. Lucas, L. T., Gatehouse, D., Jones, G. D., and Shuker, D. E. (2001) Characterization of DNA damage at purine residues in oligonucleotides and calf thymus DNA induced by the mutagen 1-nitrosoindole-3-acetonitrile, *Chem. Res. Toxicol. 14*, 158−164.
13. Suzuki, T., Yoshida, M., Yamada, M., Ide, H., Kobayashi, M., Kanaori, K., Tajima, K., and Makino, K. (1998) Misincorporation of 2′-deoxyoxanosine 5′-triphosphate by DNA polymerases and its implication for mutagenesis, *Biochemistry 37*, 11592−11598.
14. Suzuki, T., Matsumura, Y., Ide, H., Kanaori, K., Tajima, K., and Makino, K. (1997) Deglycosylation susceptibility and base-pairing stability of 2′-deoxyoxanosine in oligodeoxynucleotide, *Biochemistry 36*, 8013−8019.
15. Nakano, T., Terato, H., Asagoshi, K., Masaoka, A., Mukuta, M., Ohyama, Y., Suzuki, T., Makino, K., and Ide, H. (2003) DNA-protein cross-link formation mediated by oxanine: a novel genotoxic mechanism of nitric oxide-induced DNA damage, *J. Biol. Chem. 278*, 25264−25272.
16. Suzuki, T., Yamada, M., Ide, H., Kanaori, K., Tajima, K., Morii, T., and Makino, K. (2000) Identification and characterization of a reaction product of 2′-deoxyoxanosine with glycine, *Chem. Res. Toxicol. 13*, 227−230.
17. Hitchcock, T. M., Dong, L., Connor, E. E., Meira, L. B., Samson, L. D., Wyatt, M. D., and Cao, W. (2004) Oxanine DNA glycosylase activity from mammalian alkyladenine glycosylase, *J. Biol. Chem. 279*, 38177−38183.
18. Terato, H., Masaoka, A., Asagoshi, K., Honsho, A., Ohyama, Y., Suzuki, T., Yamada, M., Makino, K., Yamamoto, K., and Ide, H. (2002) Novel repair activities of AlkA (3-methyladenine DNA glycosylase II) and endonuclease VIII for xanthine and oxanine, guanine lesions induced by nitric oxide and nitrous acid, *Nucleic Acids Res. 30*, 4975−4984.
19. Hitchcock, T. M., Gao, H., and Cao, W. (2004) Cleavage of deoxyoxanosine-containing oligodeoxyribonucleotides by bacterial endonuclease V, *Nucleic Acids Res. 32*, 4071−4080.
20. Nakano, T., Katafuchi, A., Shimizu, R., Terato, H., Suzuki, T., Tauchi, H., Makino, K., Skorvaga, M., Van Houten, B., and Ide, H. (2005) Repair activity of base and nucleotide excision repair enzymes for guanine lesions induced by nitrosative stress, *Nucleic Acids Res. 33*, 2181−2191.
21. Barret, G. C., Ed. (1985) *Chemistry and Biochemistry of the Amino Acids*, Chapman and Hall, New York.
22. Nakamura, H., Yagisawa, N., Shimada, N., Takita, T., Umezawa, H., and Iitaka, Y. J. (1981) The X-ray structure determination of oxanosine, *J. Antibiot. 34*, 1219−1221.
23. Meister, A., and Anderson, M. E. (1983) Glutathione, *Annu. Rev. Biochem. 52*, 711−760.
24. Kosower, N. S., and Kosower, E. M. (1978) The glutathione status of cells, *Int. Rev. Cytol. 54*, 109−160.
25. Masella, R., Di Benedetto, R., Vari, R., Filesi, C., and Giovannini, C. (2005) Novel mechanisms of natural antioxidant compounds in biological systems: involvement of glutathione and glutathione-related enzymes, *J. Nutr. Biochem. 16*, 577−586.
26. Giulivi, C., Juan José Poderoso, J. J., and Boveris, A. (1998) Production of nitric oxide by mitochondria, *J. Biol. Chem. 273*, 11038−11043.
27. Brown, G. C. (1999) Nitric oxide and mitochondrial respiration, *Biochim. Biophys. Acta 1411*, 351−369.
28. Boveris, A., Costa, L. E., Poderoso, J. J., Carreras, M. C., and Cadenas, E. (2000) Regulation of mitochondrial respiration by oxygen and nitric oxide, *Ann. N.Y. Acad. Sci. 899*, 121−135.
29. Yakes, F. M., and Houten, B. V. (1997) Mitochondrial DNA damage is more extensive and persists longer than nuclear DNA damage in human cells following oxidative stress, *Proc. Natl. Acad. Sci. U.S.A. 94*, 514−519.
30. Zastawny, T. H., Dabrowska, M., Jaskolski, T., Klimarczyk, M., Kulinski, L., Koszela, A., Szczesniewicz, M., Sliwinska, M., Witkowski, P., and Olinski, R. (1998) Comparison of oxidative base damage in mitochondrial and nuclear DNA, *Free Radical Biol. Med. 24*, 722−725.
31. Hamilton, M. L., Guo, Z., Fuller, C. D., Van Remmen, H., Ward, W. F., Austad, S. N., Troyer, D. A., Thompson, I., and Richardson, A. (2001) A reliable assessment of 8-oxo-2-deoxyguanosine levels in nuclear and mitochondrial DNA using the sodium iodide method to isolate DNA, *Nucleic Acids Res. 29*, 2117−2126.
32. Croteau, D. L., and Bohr, V. A. (1997). Repair of oxidative damage to nuclear and mitochondrial DNA in mammalian cells, *J. Biol. Chem. 272*, 25409−25412.
33. Lim, K. S., Jeyaseelan, K., Whiteman, M., Jenner, A., and Halliwell, B. (2005) Oxidative damage in mitochondrial DNA is not extensive, *Ann. N.Y. Acad. Sci.* 1042, 210−220.
34. Penta, J. S., Johnson, F. M., Wachsman, J. T., and Copeland, W. C. (2001) Mitochondrial DNA in human malignancy, *Mutat. Res. 488*, 119−133.
35. Birch-Machin, M A. (2005) Using mitochondrial DNA as a biosensor of early cancer development, *Br. J. Cancer 93*, 271−272.
36. Shimada, N., Yagisawa, N., Naganawa, H., Takita, T., Hamada, M., Takeuchi, T., and Umezawa, H. J. (1981) Oxanosine, a novel nucleoside from actinomycetes, *J. Antibiot. 34*, 1216−1218.
37. Yagisawa, N., Shimada, N., Takita, T., Ishizuka, M., Takeuchi, T., and Umezawa, H. J. (1982) Mode of action of oxanosine, a novel nucleoside antibiotic, *J. Antibiot. 35*, 755−759.
38. Fornace, A. J., Jr., and Little, J. B. (1980) Malignant transformation by the DNA−protein crosslinking agent trans-Pt(II) diamminedichloride, *Carcinogenesis 1*, 989−994.
39. Fornace, A. J., Jr. (1982) Detection of DNA single-strand breaks produced during the repair of damage by DNA−protein cross-linking agents, *Cancer Res. 42*, 145−149.
40. Bradley, M. O., Hsu, I. C., and Harris, C. C. (1979) Relationship between sister chromatid exchange and mutagenicity, toxicity, and DNA damage, *Nature 282*, 318−320.
41. Bradley, M. O., and Kohn, K. W. (1979) X-ray induced DNA double strand break production and repair in mammalian cells as measured by neutral filter elution, *Nucleic Acids Res. 7*, 793−804.
42. Merk, O., and Speit, G. (1998) Significance of formaldehyde-induced DNA−protein crosslinks for mutagenesis, *Environ. Mol. Mutagen. 32*, 260−268.
43. McKnight, G. M., Smith, L. M., Drummond, R. S., Duncan, C. W., Golden, M., and Benjamin, N. (1997) Chemical synthesis of nitric oxide in the stomach from dietary nitrate in humans, *Gut 40*, 211−214.
44. Licht, W. R., Fox, J., and Deen, W. M. (1988) Effects of ascorbic acid and thiocyanate on nitrosation of proline in the dog stomach, *Carcinogenesis 9*, 373−377.
45. Licht, W. R., Tannenbaum, S. R., and Deen, W. M. (1988) Use of ascorbic acid to inhibit nitrosation: kinetic and mass transfer considerations for an *in vitro* system, *Carcinogenesis 9*, 365−372.
46. Xu, J., Xu, X., and Verstraete, W. (2001) The bactericidal effect and chemical reactions of acidified nitrite under conditions simulating the stomach, *J. Appl. Microbiol. 90*, 523−529.
47. Takahama, U., Yamamoto, A., Hirota, S., and Oniki, T. (2003) Quercetin-dependent reduction of salivary nitrite to nitric oxide under acidic conditions and interaction between quercetin and ascorbic acid during the reduction, *J. Agric. Food Chem. 51*, 6014−6020.

48. Bartsch, H., Ohshima, H., Pignatelli, B., and Carmels, S. (1992) Endogenously formed *N*-nitroso compounds and nitrosating agents in human cancer aetiology, *Pharmacogenetics 2*, 227−277.
49. Choi, N. W., Miller, A. B., Fodor, J. G., Jain, M., Howe, G. R., Risch, H. A., and Ruder, A. M. (1987) Consumption of precursors of *N*-nitroso compounds and human gastric cancer, *IARC Sci. Publ. 84*, 492−496.
50. Lewis, R. S., Tannenbaum, S. R., and Deen, W. M. (1995) Kinetics of *N*-nitrosation in oxygenated nitric oxide solutions at physiological pH: Role of nitrous anhydride and effects of phosphate and chloride, *J. Am. Chem. Soc. 117*, 3933−3939.
51. Ischiropoulos, H., Zhu, L., and Beckman, J. S. (1992) Peroxynitrite formation from macrophage-derived nitric oxide, *Arch. Biochem. Biophys. 298*, 446−451.
52. Beckman, J. S., Beckman, T. W., Chen, J., Marshall, P. A., and Freeman, B. (1990) Apparent hydroxyl radical production by peroxynitrite: Implications for endothelial injury from nitric oxide and superoxide, *Proc. Natl. Acad. Sci. U.S.A. 87*, 1620−1624.
53. World Health Organization. (1977) *"Oxides of Nitrogen", WHO Environ. Health Criteria 4.*
54. Dong, M., Wang, C., Deen, W. M., and Dedon, P. C. (2003) Absence of 2′-deoxyoxanosine and presence of abasic sites in DNA exposed to nitric oxide at controlled physiological concentrations, *Chem. Res. Toxicol. 16*, 1044−1055.
55. Dong, M., and Dedon, P. C. (2006) Relatively small increases in the steady-state levels of nucleobase deamination products in DNA from human TK6 cells exposed to toxic levels of nitric oxide, *Chem. Res. Toxicol. 19*, 50−57.

BI0620398